Effect of percolation on thermal transport in nanotube composites

S. Kumar[a)]
School of Mechanical Engineering, Purdue University, West Lafayette, Indiana 47907

M. A. Alam
School of Electrical and Computer Engineering, Purdue University, West Lafayette, Indiana 47907

J. Y. Murthy
School of Mechanical Engineering, Purdue University, West Lafayette, Indiana 47907

(Received 29 October 2006; accepted 4 February 2007; published online 9 March 2007)

The effective thermal conductivity of two-dimensional (2D) nanocomposites composed of carbon nanotubes (CNTs) dispersed in a host substrate is simulated to quantify the role of tube percolation on the thermal transport. The model is in excellent agreement with a 2D effective medium theory for low tube densities, but departs significantly from it when tube-tube interaction becomes significant. It is found that percolation effects may play a role for tube-tube and tube-substrate thermal resistance parameters typical of CNT composites. They are quantified in terms of a conductivity exponent for a range of governing parameters. © *2007 American Institute of Physics*.
[DOI: 10.1063/1.2712428]

In recent years, carbon nanotube (CNT)-based composites have been investigated intensively in diverse applications including macroelectronics,[1–7] thermal management,[8–10] and high strength materials.[11] In these applications, CNTs are randomly dispersed in a host substrate and may form a percolating network even at low volume fractions ($\sim$0.2%) due to their high aspect ratio.[4,10] Heat exchange with the substrate through the large lateral contact area has been assumed to diminish the role of percolation in determining composite thermal conductivity.[12] Therefore, most published theoretical research[9,13–15] does not account for percolation, including widely used effective medium approximations.[16] However, recent studies of thermal contact resistance have shown that tube-substrate and tube-tube contact resistances are both very high.[12,17,18] If the soft contact between the tube and the substrate is resistive enough to dominate the high tube-tube resistance, network percolation may play a role in thermal transport. Though a few recent publications[19–21] have accounted for percolation in nanotube networks, none have considered the role of these competing effects, and nearly all address three-dimensional (3D) bulk composites.

The focus of this letter is thermal transport in two-dimensional (2D) thin-film CNT composites used in flexible macroelectronics and organic electronics.[2–4,6,7] Our objectives are (i) to establish the limits of the traditional effective medium approximation[15,16] (EMA) in analyzing the effective thermal conductivity of 2D CNT composites and (ii) to identify the range of contact parameters for which percolation could play a role in thermal transport. We demonstrate that 2D EMA underpredicts effective thermal conductivity (k_{eff}) even at tube densities well below the percolation threshold. We show that the role of percolation depends critically on the strength of tube-to-substrate and tube-to-tube contact resistances for large enough tube-to-substrate conductivity ratio, and that percolation could play a role for resistance values that fall within the range of published measurements. We quantify the importance of percolation effects by determining the conductivity exponent as a function of tube density.

We represent the CNT network composite [see inset in Fig. 1(b)] as a 2D random network of nanotubes of length L_t and diameter d dispersed in a matrix of length L_C, width H, and thickness t. Since $L_t/d \gg 1$, there are sufficient phonon boundary scattering events at the substrate-tube interface that classical Fourier conduction obtains in both tube and substrate.[6,22] Assuming one-dimensional diffusive transport along the nondimensional length s^* of the tube, three-dimensional conduction in the substrate, and heat transfer

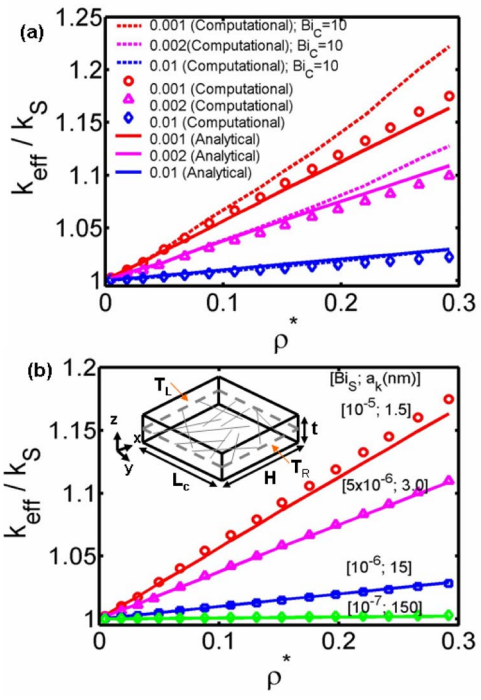

FIG. 1. (Color online) (a) Comparison of normalized effective thermal conductivity (k_{eff}/k_S) computed from numerical simulations and analytically derived expressions for different k_S/k_t ratios. $L_C/L_t=8$ ($L_t=0.5$ μm), $H/L_t=4$, $\text{Bi}_S=10^{-5}$, and $\rho^*=0-0.3$ ($\rho=0.1-6.5$ μm^{-2}). $\text{Bi}_C=0$ for simulations unless otherwise stated. (b) Comparison of normalized effective thermal conductivity (k_{eff}/k_S) computed from numerical simulations and 2D EMA for different values of the interfacial thermal resistance Bi_S ($10^{-7}-10^{-5}$) for $\text{Bi}_C=0$. $L_C/L_t=8$ ($L_t=0.5$ μm), $H/L_t=4$, $k_S/k_t=10^{-3}$, and $\rho^*=0-0.3$ ($\rho=0.1-6.5$ μm^{-2}).

[a)]Electronic mail: kumar21@purdue.edu

between intersecting tubes as well as to the substrate, the governing nondimensional energy equations in the tube and substrate may be written, respectively, as

$$\frac{d^2\theta_i}{ds^{*2}} + \sum_{\text{intersecting tubes j}} \text{Bi}_C(\theta_j - \theta_i) + \text{Bi}_S(\theta_S - \theta_i) = 0, \quad (1a)$$

$$\nabla^{*2}\theta_S + \sum_{i=1}^{N_{\text{tubes}}} \text{Bi}_S \beta_v \frac{k_t}{k_s}(\theta_i - \theta_S) = 0. \quad (1b)$$

Here, $\theta=(T-T_L)/(T_L-T_R)$, where T_L and T_R are the boundary temperatures [see inset in Fig. 1(b)], and all lengths are nondimensionalized by the tube diameter d. Here, Bi_C represents the dimensionless tube-to-tube contact conductance and Bi_S represents the dimensionless tube-substrate contact conductance.[9] k_S/k_t is the ratio of the substrate and tube conductivities and $\rho^*(=\rho/\rho_{\text{th}})$ is the dimensionless tube density, where $\rho_{\text{th}}(=4.23^2/\pi L_t^2)$ (Refs. 4 and 22) is the density at the global percolation threshold. Other details are given in Ref. 23. The problem is solved numerically using the finite volume method;[6,24] 100 random realizations are used to obtain a statistically significant result.

For low-density ellipsoid dispersions, the effective conductivity (k_{eff}) has been derived in Ref. 16 using a Maxwell-Garnett EMA. For a planar CNT network, isotropic in the x-y plane [see inset in Fig. 1(b)] and embedded in a substrate of thickness d, the theory in Ref. 16 may be modified to yield k_{eff} in the x-y plane as

$$k_x = k_y = k_S \frac{2 + f[\beta_{11}(1 - L_{11}) + \beta_{33}(1 - L_{33})]}{2 - f[\beta_{11}L_{11} + \beta_{33}L_{33}]}. \quad (2)$$

Here f is the volume fraction, L_{ii} is the depolarization factor, and $\beta_{ii}=(k_{ii}-k_S)/[k_S+L_{ii}(k_{ii}-k_S)]$, $k_{11}=k_{22}=k_t/[1+(2a_K k_t/k_S d)]$, and $k_{33}=k_t/[1+(2a_K k_t/k_S L_t)]$. Here, a_K is the Kapitza radius,[9,16] axis 3 represents the longitudinal axis of the CNT, and axes 1 and 2 are the other two axes of the CNT.[16]

The finite volume computation of k_{eff} is compared with predictions from the 2D EMA in Figs. 1(a) and 1(b). For this case, the polarization factors are given by $L_{11}=L_{22}=0.5$, $L_{33}=0$. Equation (2) assumes that ρ is very low, and that the tubes do not interact with each other. Consequently, the tube-tube contact parameter Bi_C is set to zero in the finite volume computations. Since the parameter Bi_S is not known *a priori*, its value is adjusted to match the results from EMA for a value of $a_K=1.5$ nm for $k_S/k_t=10^{-2}$. The same value of Bi_S is used in all subsequent calculations for other k_S/k_t ratios in Fig. 1(a). A good match with the results of EMA is obtained for the case of $\text{Bi}_C=0$. Calculations were also performed in Fig. 1(a) for $\text{Bi}_C=10$, representing nearly perfect contact. For high Bi_C, the numerically computed k_{eff} is observed to deviate substantially from the EMA prediction even for densities below ρ_{th}. This deviation is significant for all but the highest k_S/k_t values ($<10^{-2}$), and would therefore be significant for computations of electrical and thermal conductivities in CNT composites. This suggests that high aspect ratio tubes interact with each other even at tube densities well-below ρ_{th} and that the EMA may be inadequate for the prediction of k_{eff} at all but the very lowest densities if tube-tube contact is sufficiently good.

Figure 1(b) presents the variation of k_{eff} with tube density with Bi_S as a parameter for $\text{Bi}_C=0$; the ratio $(1/a_K)/\text{Bi}_S$ is held constant in the figure. A good match with EMA is found, indicating that a_K and Bi_S are consistent. The results in Fig. 1 indicate that adjusting a_K to fit experimental data in previous studies[9,25] adjusts in part for tube-tube interaction effects not present in EMA theory. These adjustments would tend to underpredict the true value of interface resistance, a claim also supported by Ref. 26. Furthermore, we have replicated the experimentally observed electrical properties in carbon-nanotube-dispersed organic thin-film transistors[27] using this model.

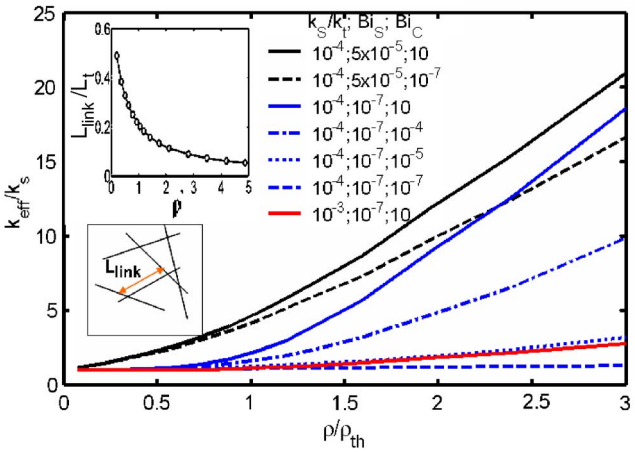

FIG. 2. (Color online) Variation of normalized effective thermal conductivity (k_{eff}/k_S) against normalized tube density ($\rho^*=\rho/\rho_{\text{th}}$) is shown for different $k_S/k_t=10^{-4}$, 10^{-3}, $\text{Bi}_S=10^{-7}$, 5×10^{-5}, and a range of Bi_C. $L_C/L_t=3$ ($L_t=2.0$ μm), $H/L_t=2$.

Figure 2 shows k_{eff} as a function of ρ. When $\rho \ll \rho_{\text{th}}$ $(=4.23^2/\pi L_t^2 \sim 1.4\ \mu\text{m}^{-2})$, k_{eff} increases linearly with ρ since the tubes do not interact either directly or through the substrate, consistent with EMA theory. This is evident in the average link length (L_{link}) vs ρ^* plot (inset in Fig. 2), where $L_{\text{link}}/L_t \sim 1$ for $\rho^* \ll 1$. Near the percolation threshold $\rho \sim \rho_{\text{th}}$, k_{eff} varies nonlinearly with ρ as expected;[2,6] a change in the slope of the curve is indicative of percolation. For $\rho > 3.0\rho_{\text{th}}$ and for large enough L_C/L_t, k_{eff} is found to vary linearly with ρ. The reason for this is evident in the inset in Fig. 2, which shows that the average L_{link} varies linearly with ρ^* for high densities ($\rho^* > 3$). In the absence of a substrate, k_{eff} is given by $k_{\text{eff}}/k_t \sim \rho L_t^2(0.783 - 0.119\ln(\text{Bi}_C^2) - 0.015\ln(\text{Bi}_C))$ for high densities.[6] For CNT composites, this expression would also depend on Bi_S and k_S/k_t, but linearity with respect to density would nevertheless be valid.

Percolation effects are evident in Fig. 2 in the change of slope of the curves near $\rho^* \sim 1$. When Bi_S is high, percolation effects are least important (black curves). When Bi_S is low, percolation effects are most important (blue curves). In spite of low Bi_S and high Bi_C, percolation may not be important if k_S/k_t is high (red curve). The spread in the curves with respect to Bi_C is greatest for low Bi_S (blue curves) and less pronounced for higher Bi_s (black curves). This spread would not be captured by EMA, which does not account for the influence of tube-tube contact. The experiments of Ref. 28 indicate that $\text{Bi}_S \sim 10^{-5}$ for CNTs in organic liquids, though no experimental data are available for CNT dispersions in plastics or organic solids. The computations of Refs. 17 and 18 indicate that $\text{Bi}_C \sim 10^{-5}$, but in the absence of experimental corroboration, these values are not definitive, and only

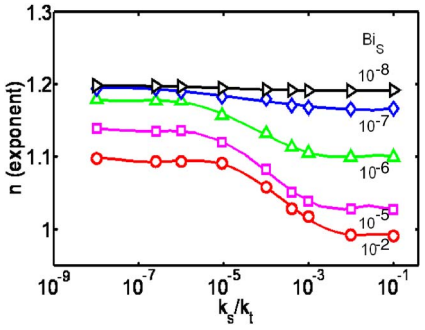

FIG. 3. (Color online) Variation of conductivity exponent (n) with k_S/k_t for different interfacial resistances Bi_S. $L_C/L_t=3$ ($L_t=2.0$ μm), $H/L_t=2$, $Bi_C=10$.

indicate the broad order of magnitude. Nevertheless, for the type of soft contact encountered in these composites, with Bi_S in the range of $10^{-5}-10^{-7}$ and Bi_C in the range of $10^{-4}-10^{-5}$, Fig. 2 indicates that percolation could play a role. However, the value of k_s/k_t is critical. For CNTs in polymer, $k_s/k_t \sim 10^{-4}$ if $k_s \sim 0.1$ W/mK and $k_t \sim 10^3$ W/mK, commensurate with freestanding CNT values. However, if k_t is significantly reduced because of phonon scattering at the tube-substrate boundary, Fig. 2 indicates that percolation effects would not be visible, and that predicted k_{eff}/k_s would be low. Effective thermal conductivity values reported in the literature for 3D composites all have $k_{\text{eff}}/k_s < 3$ or so, in contrast to some of the high values seen in Fig. 2, indicating that k_t reduction due to interface scattering could play a significant role.

Electrical transport in the linear regime in CNT organic composites may be analyzed using a model similar to that for thermal transport.[27] Figure 2 indicates that strong nonlinear behavior near the percolation threshold would be observed for electrical (charge) transport in CNT-polymer composites due to very low $k_S/k_t(<10^{-6})$,[2,6] low Bi_S, and high Bi_C.[6,27]

The effect of Bi_S and k_S/k_t on percolation behavior is quantified by computing the conductivity exponent n, given by $k_{\text{eff}}-k_{\text{eff,th}} \sim (\rho-\rho_{th})^n$ in Fig. 3; it is computed for $(\rho_{\text{th}} < \rho < 2^*\rho_{\text{th}})$.[29–31] For high tube-substrate thermal resistance ($Bi_S \sim 10^{-8}$), n is nearly constant at a value of 1.2, close to the 2D exponent of 1.3 Refs. 29 and 30 for the pure network. The value of this exponent depends on L_C/L_t and is expected to tend to 1.3 when L_C/L_t is sufficiently large. With increasing Bi_S, the variation in n with k_S/k_t becomes significant. For high Bi_S and high k_S/k_t, n is close to 1.0, so that the medium behaves like a linear resistor and percolation effects are completely suppressed. When k_S/k_t is decreased at high Bi_S, n increases until $k_S/k_t \sim 10^{-6}$, but attains a constant value for $k_S/k_t < 10^{-6}$, indicating that percolation effects are becoming more pronounced. This muting of the effects of network percolation at high Bi_S has been observed in electrical measurements of current-voltage characteristics (I_D-V_G curves)[7] in CNT-organic transistors. However, the conductivity exponents in Fig. 3 are not universal and are sensitive to many factors including d/L_t, L_C/L_t, and Bi_C.

In summary, a computational diffusive transport model is used to explore the thermal conductivity of 2D nanotube composites and the dependence of percolation behavior on Bi_C, Bi_S, and k_S/k_t. Numerical predictions are in excellent agreement with theoretical EMA-based results in the extremely low volume fraction limit, but depart from EMA for higher volume fractions below the percolation limit because of tube-tube interaction. The effective thermal conductivity varies linearly with ρ in the low and high density regimes (explained by the average L_{link}), while nonlinear behavior near ρ_{th} is found for low k_S/k_t, low Bi_S, and high-enough Bi_C. This analysis of percolation effects will help interpret and guide the future experiments on nanocomposites for a wide range of practical applications.

[1] X. F. Duan, C. M. Niu, V. Sahi, J. Chen, J. W. Parce, S. Empedcoles, and J. L. Goldman, Nature (London) **425**, 274 (2003).
[2] E. S. Snow, J. P. Novak, P. M. Campbell, and D. Park, Appl. Phys. Lett. **82**, 2145 (2003).
[3] Y. X. Zhou, A. Gaur, S. H. Hur, C. Kocabas, M. A. Meitl, M. Shim, and J. A. Rogers, Nano Lett. **4**, 2031 (2004).
[4] L. Hu, D. S. Hecht, and G. Gruner, Nano Lett. **4**, 2513 (2004).
[5] R. V. Seidel, A. P. Graham, B. Rajasekharan, E. Unger, M. Liebau, G. S. Duesberg, F. Kreupl, and W. Hoenlein, J. Appl. Phys. **96**, 6694 (2004).
[6] S. Kumar, J. Y. Murthy, and M. A. Alam, Phys. Rev. Lett. **95**, 066802 (2005).
[7] X. Z. Bo, C. Y. Lee, M. S. Strano, M. Goldfinger, C. Nuckolls, and G. B. Blanchet, Appl. Phys. Lett. **86**, 182102 (2005).
[8] H. Huang, C. Liu, Y. Wu, and S. Fan, Adv. Mater. (Weinheim, Ger.) **17**, 1652 (2005).
[9] C. W. Nan, G. Liu, Y. Lin, and M. Li, Appl. Phys. Lett. **85**, 3549 (2004).
[10] M. J. Biercuk, M. C. Llaguno, M. Radosavljevic, J. K. Hyun, A. T. Johnson, and J. E. Fischer, Appl. Phys. Lett. **80**, 2767 (2002).
[11] X. J. Xue and M. M. Thwe, Appl. Phys. Lett. **81**, 2833 (2002).
[12] N. Shenogin, S. Shenogin, L. Xue, and P. Keblinski, Appl. Phys. Lett. **87**, 133106 (2005).
[13] D. P. H. Hasselman and L. F. Johnson, J. Comput. Math. **21**, 509 (1986).
[14] Y. Benveniste and T. Miloh, J. Appl. Phys. **69**, 1337 (1991).
[15] C. W. Nan, Z. Shi, and M. Lin, Chem. Phys. Lett. **375**, 666 (2003).
[16] C. W. Nan, R. Berringer, D. R. Clarke, and H. Gleiter, J. Appl. Phys. **81**, 6692 (1997).
[17] H. L. Zhong and J. R. Lukes, Phys. Rev. B **74**, 125403 (2006).
[18] S. Maruyama, Y. Igarashi, Y. Taniguchi, and Y. Shibuta, First International Symposium on Micro and Nanotechnlogy, Hawaii, March 2004 (unpublished).
[19] P. Keblinski and F. Cleri, Phys. Rev. B **69**, 184201 (2004).
[20] M. Foygel, R. D. Morris, D. Anez, S. French, and V. L. Sobolev, Phys. Rev. B **71**, 104201 (2005).
[21] T. Hu, A. Y. Grosberg, and B. I. Shklovskii, Phys. Rev. B **73**, 155434 (2006).
[22] S. Kumar, N. Pimparkar, J. Y. Murthy, and M. A. Alam, Appl. Phys. Lett. **88**, 123505 (2006).
[23] The geometric parameter β_v is given by $\beta_v=\alpha_v A_t/P_S$, where α_v is the contact area of the tube per unit volume of the substrate, A_t is cross-section area of tube, and P_S is perimeter of tube. Boundary conditions $\theta_t=1.0$ and $\theta_t=0$ are applied to tube tips touching left and right faces of substrate, respectively. All the tube tips terminating inside the substrate are assumed adiabatic. The boundary conditions for the substrate are given by $\theta_S=1$ at $x^*=0$; $\theta_S=0$ at $x^*=L_C/d$, and $\partial\theta_S/\partial z^*=0$ at $z^*=0$ and at $z^*=t/d$ [see inset in Fig. 1(b)]. The boundaries $y^*=0$ and $y^*=H/d$ are assumed to be periodic boundaries for both substrate and tubes.
[24] S. V. Patankar, *Numerical Heat Transfer and Fluid Flow* (Hemisphere, New York, 1980).
[25] M. B. Bryning, D. E. Milkie, M. F. Islam, J. M. Kikkawa, and A. G. Yodh, Appl. Phys. Lett. **87**, 161909 (2005).
[26] M. T. Hung, O. Choi, Y. S. Ju, and H. T. Hahn, Appl. Phys. Lett. **89**, 023117 (2006).
[27] S. Kumar, G. B. Blanchet, M. S. Hybertsen, J. Y. Murthy, and M. A. Alam, Appl. Phys. Lett. **89**, 143501 (2006).
[28] S. T. Huxtable, D. G. Cahill, S. Shenogin, L. Xue, R. Oziski, P. Barone, M. Usrey, M. S. Strano, G. Siddons, M. Shim, and P. Keblinski, Nat. Mater. **2**, 731 (2003).
[29] C. J. Lobb and D. J. Frank, Phys. Rev. B **30**, 4090 (1984).
[30] D. J. Frank and C. J. Lobb, Phys. Rev. B **37**, 302 (1988).
[31] D. Stauffer and A. Aharony, *Introduction to Percolation Theory* (Taylor & Francis, London, 1994), pp. 89–99.